Department of Commerce
Weather Bureau
Office of Hydrologic Director

War Department
Corps of Engineers
Engineer Department

Hydrometeorological Report No. 21B

Revised Report

on

Maximum Possible Precipitation

Los Angeles Area, California

Prepared by

The Hydrometeorological Section

Office of Hydrologic Director

December 29, 1945

FOREWORD

A "Preliminary Report on Maximum Possible Precipitation, Los Angeles Area, California" was issued by the Hydrometeorological Section, in cooperation with the Corps of Engineers, on December 30, 1944. Since then, further consultations with the Los Angeles District Engineer Office have disclosed the need for certain revisions, among them a specific differentiation between the estimates of the maximum general and the maximum local storms for the region. The Revised Report now issued supersedes the Preliminary Report. It contains not only the revisions requested but also the pertinent results of recent evolutionary changes in hydrometeorological technique.

Major Los Angeles Storms

1. The dominating influences on the weather of the entire West Coast are the semipermanent pressure centers over the ocean which develop from the general circulation of the atmosphere. The mean positions of these semipermanent low- and high-pressure centers are at about 55°N and 35°N, respectively. Following the annual march of the solar altitude, these pressure systems are farthest south in the winter and farthest north in the summer. The low-pressure system is usually referred to as the Aleutian Low and the high-pressure system as the Pacific High of the North Pacific Ocean. A full discussion of the seasonal variation in strength, extent, position, and general characteristics of these semipermanent centers of action is given in chapter II, Dynamic Climatology, of Hydrometeorological Report No. 3, "Maximum Possible Precipitation over the Sacramento Basin of California."

2. The rainy season, or season during which major storms occur over southern California, is November through April. The southward displacement of both semipermanent centers of action during this period, together with a similar displacement of the polar front and the mean storm track, brings southern California under the influence of cyclonic systems moving inland from the Pacific. Storms which produce appreciable rain anywhere along the Pacific Coast of the United States may be divided into types, but all types will have some important features in common, except the decadent tropical storms which infrequently move far enough north to affect southern California. Basically, the location, intensity, moisture charge, and movement of the centers of low pressure are the factors which make any storm a flood-producing storm for a particular section of the

Pacific Coast region. Chapter V of the Sacramento Report describes fully the major features of flood-producing storms for the Sacramento Basin and these are applicable also to flood-producing storms over southern California.

3. Ten of the major storms of record over southern California have been subjected to a critical analysis to determine whether or not there was any similarity in the general features of the storms. The weather map concurrent with the period of greatest precipitation has been used as the primary basis for comparison. In general, all storms which produce appreciable amounts of precipiation over this area have similar characteristics. Cyclonic systems which result in gradient winds from the southwest quadrant over southern California produce precipitation, and intensity of precipitation varies directly with wind velocity and dewpoint but inversely with distance of the cyclonic system from the area. The air masses involved differ only slightly in their essential characteristics. Over large areas the effect of frontal activity on depth of precipitation is unimportant except that the passage of a well-defined cold or occluded front ends any appreciable accumulation of average depth. Over small areas, however, the frontal passage may contribute a marked increase in depth because of the heavier local precipitation occurring along the trough line with its intensifying effect on convergence.

4. Nine of the storms analyzed occurred with, or following, the southward push of a cold polar air mass into the Mississippi and Missouri Valleys. In most cases the storm developed off the West Coast when the cold air had spread westward over the Rocky Mountains into the Great Basin and the northwest states. Associated with the large mass of cold air over the continent was a widespread high-pressure area which in every case

extended northwestward into Alaska and the polar region. In each storm the highest pressure exceeded 1025 millibars; during the storms of February 1927, December 1933-January 1934, and December 1921, and the two January 1916 storms, it exceeded 1040 millibars. The temperatures in the polar air were generally well below the average minimum temperatures for the season of the year, ranging from about 10°F as the polar air spread southward into the Dakotas in the April 1926 storm, to temperatures below -20°F in several of the midwinter storms. On the basis of pressure patterns, the nine storms mentioned above can be divided into two general classes. In class 1, a low-pressure area extended from California westward or northwestward beyond the Aleutian Islands and included two or more separate and well-developed centers. In class 2, a large area of low pressure was centered off the West Coast, bounded on the east and west by extensive high-pressure systems which were connected on the north by a high-pressure ridge. The high pressure on the west was usually centered over the Gulf of Alaska and extended far southward, deep into the middle latitudes.

5. The storms of January 20-24, 1943, February 27-March 4, 1938, December 30, 1933 - January 1, 1934, February 13-16, 1927, April 4-9, 1926, and February 17-22, 1914, are class 1 storms. Precipitation in these storms occurred in two periods associated with the passage of two cyclonic systems which moved in over the coast in close succession from a westerly direction, but curved toward the southeast as they moved inland. The second cyclonic system was usually the more intense and produced the heavier rainfall. The first system moved inland and occluded against the high mountains before any appreciable amount of the cold polar continental

air had spilled westward into the northern coastal region. The first system thus set up the circulation for injecting large amounts of polar air into the developing secondary system which followed, providing the energy for the more intense second development.

6. Storms in class 2 are those of December 18-27, 1921, January 14-19, 1916, and January 24-29, 1916. The pressure distribution over the United States during these storms resulted in a relatively slow translation of the systems eastward. In the first stages the low-pressure area usually developed off the coast of British Columbia, moved south or south-southeastward, passed inland over Oregon or northern California, and then moved in a more eastward direction. As in class 1, a secondary storm followed. However, it was the first storm which caused the cold air on the east and north to push southward over the northwest states. Thus, the second storm moved in a path farther to the south along the polar front and inland over central California. As in class 1 storms, more cold air was drawn into the second, and usually more intense, system than into the first. The heavier rainfall was again associated with the second disturbance.

7. The tenth storm, that of February 13-15, 1937, was associated with a wave which developed February 11 on a Pacific front at about longitude 145°W and latitude 30°N. As this wave disturbance moved toward the central California coast on the 13th, a strong southeast-northwest pressure gradient was established over southern California, causing strong southwest winds. The storm precipitation, of relatively short duration and high intensity, occurred over southern California during the night of the 13th-14th and was associated with the movement of this disturbance inland over the area. The only similarity between the general pressure distribution of this storm and that of the other nine major storms is that a strong southeast-northwest pressure gradient was established over southern California.

The Maximum Possible Storm

8. As stated previously, results from a detailed analysis of all the storms show that the major rainfall occurs with a combination of high wind and high dewpoints. Therefore, in any attempt to reproduce mass curves of rainfall over this area, wind and dewpoint must be considered the primary controlling factors, the dewpoint being a measure of the precipitable water, as explained in Hydrometeorological Report No. 3.

9. The steepest pressure gradients of record between San Francisco and Los Angeles, and the highest winds of record at San Diego and Los Angeles, were observed in the storms of January 24-29, 1916, and January 20-24, 1943. Upper-air observations were available for only the latter of the two storms and during this period the temperatures at the 3- and 5-kilometer levels over the northwest states equaled, or approached, the minima of record. Simultaneously, the temperatures at these levels over San Diego were within 5 to 10°C of the maxima of record. Since sea-level pressure gradients during this storm were the steepest of record and the temperature gradients aloft undoubtedly approached the maximum of record, there is little reason to believe that these gradients can be exceeded by any appreciable amount. Very extreme conditions would be required to produce wind movement as much as 10% in excess of that observed in the January 1943 storm.

10. A theoretical method of determining the maximum possible precipitation over an area in a given time was developed in chapters I and II of Hydrometeorological Report No. 2, "Maximum Possible Precipitation over the Ohio River Basin above Pittsburgh, Pennsylvania, " and in chapter VI of the Sacramento Report. Also, reference was made to this method in a recent paper, "An Approach to Quantitative Forecasting of Precipitation,

Part II - Formulas for Quantitative Rainfall Forecasting " by A. K. Showalter. The latter paper demonstrates that rainfall formulas are most readily derived by means of a storage equation in which the inflow minus the outflow of moisture equals storage or amount precipitated. For the computation the following assumptions are made:

1. The rain occurs over a finite rectangular area XY, with X normal to both inflow and outflow, and Y parallel to inflow and outflow.
2. There is no net convergence of air upon the area, except for the water vapor precipitated, which amounts to no more than one or two percent of the mass of air involved.
3. There are no horizontal velocity gradients within the vertical planes normal to inflow or outflow.
4. The depths of inflow and outflow can each be defined as a pressure difference constant along X.
5. The air throughout is saturated and has a pseudo-adiabatic lapse rate.

11. In a steady state, inflow mass transport and outflow mass transport will be equal except for the negligible loss of water vapor by precipitation, or

$$V_1 M_1 = V_2 M_2$$

where subscripts 1 and 2 refer to inflow and outflow, respectively, and V and M to velocity and mass, respectively. The mass in grams per unit column of cm^2 cross-section is

$$m = \Delta p/g$$

since Δp is in millibars, which are dynes cm^{-2}. Neglecting variations in g (acceleration of gravity)

$$m = 1.02 \Delta p$$

The specific humidity q (gm/gm) is the percentage of the mass of air that is water vapor, so that mass of water vapor per unit column is

$$m_w = \int_0^z q\, dm = 1.02 \int_0^z q\, dp$$

or, approximately, $1.02\ \bar{q}\ \Delta p$

Since a gram of liquid water per cm^2 cross-section has a depth of one cm, the depth of precipitable water in cm in a unit column is also

$$1.02\ \bar{q}\ \Delta p$$

Converted to inches this depth becomes

$$W_p = .4\ \bar{q}\ \Delta p$$

In the W_p chart (figure 3), where W_p is a function of the dewpoint at 1000 mb, the computations have been made for values of Δp small enough to eliminate all but negligible errors.

12. The transport of water vapor by each unit column is thus

$$.4\ V\ \bar{q}\ \Delta p$$

and the total number of unit columns crossing a given line normal to V is XY. The storage equation of water vapor thus becomes

$$R = \frac{.4V_1X\ \bar{q}\ \Delta p_1 - .4V_2X\ \bar{q}_2 \Delta p_2}{XY} \qquad (1)$$

which is dimensionally correct if it is remembered that Δp has been previously converted to units of mass (grams). R is thus the average depth of precipitation, in inches per hour, over XY. Furthermore, Since $M_1V_1 = M_2V_2$ and therefore

$$1.02 \Delta p_1 V_1 = 1.02\ \Delta\ p_2 V_2$$

$$V_2 = \frac{\Delta p_1 V_1}{\Delta p_2}$$

and since $.4\ \bar{q} \Delta p = W_p$

the storage equation can be more simply written

$$R = \frac{V_1 \left(W_{p1} - \frac{\Delta p_1}{\Delta p_2} W_{p2}\right)}{Y} \qquad (2)$$

Previous tests have indicated that it is usually not necessary to weight the wind speed with elevation in terms of moisture content.

13. Figure 1 is a schematic illustration of one type of flow fulfilling the basic assumptions, a case of downwind deceleration. The flow of air is parallel to the planes AEFB and DHGC. Inflow and outflow are normal to the planes ADHE and BCGF. The difference between depths of inflow and outflow is representative of a hypothetical situation where, because of internal convergence, the horizontal velocity on the outflow side is equal to one-half the inflow velocity. It follows that the amount of moisture precipitated over the area ABCD in unit time is equal to the moisture inflow minus the moisture outflow in the same time. Actually the air is also being lifted above the surface EFGH, and a complete calculation would have to include one for the layer above EFGH up to the level of no lift. The computation for each layer can be made by means of equation 2.

14. In the case of the Los Angeles area, the orographic barriers determine to a great extent the general distribution of the highest amounts of rainfall. In the ten major storms there was some variation in the location of the highest centers of rainfall, but there was little variation in the location of the 10,000-square-mile area over which the maximum precipitation occurred. This fact demonstrates that the orographic features are the major controlling factors for precipitating the moisture and determining its distribution over area. However, there is one important exception: intense local rainfall associated with the convergent processes of the cyclonic system itself can and does occur over any area irrespective

of topography. In the Los Angeles area this rainfall usually has a relatively short duration (less than 12 hours); for longer periods the largest amounts of precipitation occur over the windward slopes or ridges, where precipitation continues as long as moist air flows in any direction that will force it up slope.

15. Since the orographic barriers in the Los Angeles area are the main controlling features for the production and distribution of rainfall, any rainfall equation will have to take into consideration: (1) the direction of flow relative to the barriers, (2) the height to which the air column is lifted, and (3) the amount of vertical shrinking, or downwind acceleration, which takes place in the air as it is forced up slope over the barriers. In order to apply equation 2 to the computation of maximum possible precipitation, it is first necessary to determine methods for evaluating the variables and then to test them by application to several storms which have occurred over the area. If the computed results match the observed values, the variables can then be increased to their physical upper limits and introduced into equation 2 in order to compute the maximum possible precipitation.

16. The problem of evaluating the variables in equation 2 is complicated by the orographic barriers. In the Los Angeles area, their average height above 1000 mb in terms of pressure difference is 200 mb. Figure 2 is a schematic illustration of the barrier effect on inflow and outflow velocities. It shows the orographic lift resulting in vertical convergence which is compensated by an increase in velocity of the air over the crest of the barrier. This reverses the order in figure 1, producing a greater depth of inflow layer (Δp_1) than outflow layer (Δp_2). In addition to evaluating the depth of inflow and outflow layers it is necessary to

determine the precipitable water content (W_p) of the air, the velocity of the air (V_1) into the area, and the distance (Y) which the air travels in precipitating its moisture.

17. In developing maximum possible rainstorms over various areas of the United States the Hydrometeorological Section has found it necessary to determine the maximum moisture charge possible for a column of air and to compare this value to those actually observed in storms which have produced major floods. Examination of upper-air soundings in these situations revealed that the air was near saturation from the surface to high elevations and the lapse rate of temperature was approximately pseudo-adiabatic throughout the column. During periods of excessive rainfall, therefore, it is reasonable to assume that the precipitable water in a column of air can be related to the surface dewpoint. A family of curves was developed (figure 3), giving the cumulative depths of precipitable water from a pressure of 1000 mb to any height, where the W_p values are given as functions of the surface dewpoint. However, because of the integral part played by the mountain barriers in the relationship between the precipitable water contained in the inflow columns and the precipitable water contained in the outflow columns, an examination of this factor was necessary.

18. In order to determine the effect of the mountain barriers on the wind flow across the area, velocity profiles were plotted for simultaneous pilot-balloon ascensions over Burbank (elevation 25 ft.), and Sandberg (elevation 4517 ft.). While Burbank is not on the coast, it was the only station available which could be used as reasonably representative of the coastal area. An examination of these wind profiles showed that the velocity over Sandberg averaged approximately 10% greater than over Burbank and that near 20,000 feet the velocities were about

equal. This indicates that the increase in velocity because of vertical convergence of the air as it moves over the barrier is largely damped out at about 20,000 feet. This is also an indication of the height which can be used for the inflow layer of air which will be lifted because of the topography of the region. In other words, any air above this level would receive no appreciable orographic lift and could therefore be disregarded. The average pressure at 20,000 feet is 460 mb, assuming a pseudo-adiabatic lapse rate and surface temperature and pressure of 55°F and 1000 mb respectively. On this basis the average thickness of the inflow layer (Δp_1) will be approximately 540 mb. In the Los Angeles area, the average height of the mountain barriers taken normal to a southwest wind, is approximately 6200 feet and the pressure at this level, using the same arguments as above, is approximately 800 mb. The average pressure difference between the top and the bottom of the outflow layer (Δp_2) above the barrier is therefore 340 mb.

19. The next step was the evaluation of W_{p1} and W_{p2} for use in the rainfall computation formula. Since both Δp_1 and Δp_2 were kept constant along X and Δp_1 (540 mb) extended from the 1000-mb level to the 460-mb level, W_{p1} could be obtained directly from figure 3 by reading off the W_p value at the intersection of the 460-mb line with the curve representing the selected dewpoint reduced to 1000 mb. However, Δp_2 (340 mb) extended only from the 800-mb level to the 460-mb level, so that W_{p2}, for any particular 1000-mb dewpoint, was obtained by subtracting from the W_{p1} for that dewpoint, the W_p value below the 800-mb line.

20. The problem of determining the total movement of air across the Los Angeles area was difficult because for early years no upper-wind observations were available, and even in later years none could be made during rain periods. The only other methods for getting a measure of the flow are: (1) using a wind record for an elevated station which would give a good approximation of the correct values, as was done in Hydrometeorological Report No. 3, (2) correcting a continuous wind record for a representative first-order Weather Bureau station in the area so that it would represent the average velocity of a column of air 20,000 feet high, and (3) use of the geostrophic or gradient winds obtained by drawing pressure maps for frequent intervals from original barograph records.

21. Since no consistent relationship could be found between the surface wind velocity at a first-order Weather Bureau station and upper-air velocity records made at nearby airport stations, the second method was dropped. The remaining possible measures of air movement across the area were: the geostrophic or the gradient wind, and the Mt. Wilson wind record, this being an elevated station from which good results might be expected. In order to determine the best measure of wind to be used in the equation, as well as to measure the relationship of dewpoint and wind to intensity of rainfall, correlation coefficients and regression equations were obtained for these elements for the ten storms selected. In addition to the above measures of wind movement, it was decided also to test the Los Angeles wind record for possible use as an index, since this would facilitate computations and reduce the necessary amount of work. The correlations obtained were tested for significance by using standard statistical significance tables. The regression equations were tested by an analysis of variance and by use of standard statistical

significance tables. The tests of the correlation coefficients showed that the relations between the precipitation intensity and the dewpoint, and between precipitation intensity and either the geostrophic or the gradient wind, were highly significant. However, the analysis of variance of the regression of dewpoint, geostrophic wind, gradient wind, Los Angeles wind, and Mt. Wilson wind, on the intensity, showed that the combination of dewpoint and geostrophic wind was most significant and accounted for 0.5 to 0.9 of the variation in rainfall intensity, the other measures of wind accounting for the remainder. The geostrophic wind was therefore selected as the best measure of total wind movement.

22. In order to evaluate the representativeness of the geostrophic wind as a measure of the average velocity of the total 20,000-foot column, the variation of pressure gradient and density with height must be considered. From the temperatures and pressures observed at the surface, the pressure gradient at 10,000 feet can be computed by means of figure 4. The assumption basic to the use of the chart is that of pseudo-adiabatic lapse rate, a valid assumption in major storms. In the figure, line AB represents a difference of 1°F per 10-mb pressure difference at the surface, going from a combination of higher temperature and pressure to a combination of lower temperature and pressure. This was a typical condition in all storms prior to frontal passages over the area. The 10,000-foot change in pressure gradient between two hypothetical station C and D on such a line follows:

	Surface Pressure	Surface Temperature	10,000-ft. pressure
Station D	1010 mb	55°F	695 mb
Station C	990 mb	53°F	680 mb
Difference	20 mb	2°F	15 mb

23. The ratio of pressure gradient at 10,000 feet to that at the surface is, thus, 15/20, i.e., the 10,000-foot pressure gradient is 75% of the surface gradient. The values used and computed are consistent with those observed in actual storms. The most intense rainfall occurred in all cases before the passage of the major cold front, and in the warm air preceding the front the temperature differences were small, usually of the order of 0° to 3°F. The average distribution of pressure and temperature was one of low temperature and pressure to the north and high temperature and pressure to the south. Pressure differences across the region varied from a few millibars to 27.4 mb, the latter being the average difference between San Francisco and Los Angeles for a three-hour period on January 21, 1943.

24. The geostrophic wind may be expressed as $V = \frac{G}{f\rho}$ where V is the geostrophic wind velocity, G the pressure gradient, f the parameter due to the earth's rotation - constant for any latitude - and ρ the density of the air. The ratio of the velocity at 10,000 feet to the velocity at the surface becomes

$$\frac{V_{10}}{V_s} = \frac{\rho_s G_{10}}{\rho_{10} G_s} \qquad (3)$$

where the subscripts refer to the levels. In the range of temperatures, 45 to 65°F, with surface pressure of 1010 mb and the assumption of a pseudo-adiabatic lapse rate of temperature, the ratio of the density at the surface to that at 10,000 feet is approximately 12/9. Since the average

ratio of the pressure gradient at 10,000 feet to the pressure gradient at the surface, as shown earlier, is 75/100, substitution in equation 3 gives:

$$\frac{V_{10}}{V_s} = \frac{12}{9} \cdot \frac{75}{100} = 1$$

Thus, the average condition in major storms is one which gives a geostrophic wind velocity constant with height to 10,000 feet. This is verified by the available 5000- and 10,000-foot charts, which show the isobaric curvature during major storms decreasing with height at such a rate that the isobars become almost straight at 10,000 feet, and the wind at that level approximately equal to the geostrophic wind speed indicated by the sea-level isobars.

25. Using the same basic assumption of pseudo-adiabatic lapse rate from 10,000 to 20,000 feet at stations C and D, figure 4, it can be shown that the velocity is approximately constant with height in that layer. Figure 5 shows the variation of wind velocity with height throughout the 20,000-foot depth in percent of the geostrophic wind measured at sea level. The variation of velocity with height in the lower 10,000 feet was assumed to be linear and the correction used for obtaining gradient wind was

$$V_{grad.} = 0.8\ V_{geos.}$$

This is an average correction based on a study of all the major storms, where isobaric curvature varied from approximately 300 miles to 1000 miles and the measured geostrophic velocities from 20 mph to 91 mph. By averaging the velocity of the whole column up to 20,000 feet in figure 5, an average of 95% of the geostrophic value measured at sea level is obtained. The geostrophic wind velocity is thus demonstrated to be a good measure of the required velocity.

26. Errors inherent in the reduction of high-level-station pressure to sea level made it inadvisable to determine the geostrophic wind from

isobars drawn for sea-level pressures. To eliminate as much error as possible, the sea-level pressures used were restricted to stations with elevations not more than 1200 feet above sea level. The pressures at stations above 1200 feet were reduced to their average level, all stations whose elevations exceeded the average level by more than 1000 feet being eliminated. In drawing the isobars the sea-level pressures were rigorously followed along the coast but the fixed-level pressures were used to determine the curvature and direction of the isobars extending eastward from California. Isobars of average pressure for the period 0600 to 0900 PST of February 28, 1938, are shown in figure 6. Pressures at the elevated stations are underlined and the arrows indicate the curvature and direction of the isobars over Nevada and eastern California. In each case the wind direction was taken as parallel to the average direction of the isobars over the 10,000-square-mile area of maximum rainfall and the wind velocity was computed from the pressure gradient measured normal to this direction across the extreme limits of the 10,000-square-mile area. Maps similar to figure 6 were drawn for every three-hour period during each storm analyzed.

27. In order to evaluate Y, the distance the air travels in precipitating its moisture over the area, the 10,000-square-mile area over which the maximum average rainfall occurred was delineated for each storm. This area was in approximately the same location for each of the storms, giving evidence of the importance of the orographic barrier in releasing and determining the general distribution of the major portion of the rainfall. In order to simplify computations a rectangle with a 10,000-square-mile area was adjusted to fit best the average pattern for all storms delineated by the maximum rainfall over 10,000 square miles.

Figure 6 shows the rectangle and its relation to the isohyet encompassing the 10,000 square miles of maximum average rainfall for the February-March 1938 storm. The base of this rectangle is normal to a wind direction of 211°. In order to comply with the original hypothesis of maintaining the flow of air parallel to the sides and normal to the base, in which case Y is always equal to 60 miles, it is necessary to obtain a measure of the wind component normal to the base of the rectangle. As will be seen later, it was more convenient to take the value of Y parallel to the wind direction between the base and the top of the rectangle. This is the mathematical equivalent of taking the component of the wind normal to the base of the rectangle. Thus the distance Y becomes a function of the wind direction and can be determined trigonometrically. When the wind direction is 280°, Y is equal to 167 miles, which is the length of the rectangle of best fit. The value of Y is kept constant for all directions between 280 and 292.5° since in no case would the air move over a greater average distance than the length of the rectangle in precipitating its moisture.

28. Obviously, the topography of the region is effective in producing precipitation only when the wind is blowing up slope, any down-slope motion being rain-inhibiting rather than rain-producing. Also to be considered is the fact that air coming into the southern California region from a direction other than between south-southeast (157.5°) and west-northwest (292.5°), clockwise, is either flowing down slope or is considerably drier than air coming in from those directions. Examination of all storms showed that when the wind was from any direction outside this SSE-WNW range no appreciable rain occurred and therefore all winds outside this range could be disregarded, except in cases where a front or marked trough extending in a west-to-east direction moved southward over California.

During these conditions appreciable rain could occur in the air preceding the front or trough passage even though the isobars indicated movement of air from a direction slightly north of west-northwest.

29. When marked frontal systems move into the area attended by a wind shift to northwest, rainfall occurs only over the portion of the 10,000-square-mile area in advance of the front. It is therefore necessary to multiply the right side of equation 2 by the percent of area in advance of the mean 3-hour position of the front to obtain the average rainfall over 10,000 square miles for the 3-hour period.

30. During some synoptic situations a wedge of high pressure extends into the area, producing winds from the SSE-WNW directions, up-slope over part of the area and down-slope over the remainder. During these periods the percent of the area experiencing up-slope winds was determined and the same weighting procedure followed as above.

31. Up to this point the following decisions have been made for evaluating the rain-producing factors:

1. For each 3-hour period, the geostrophic wind as measured from isobars carefully drawn from the 3-hour average pressures will be used for V_1, the inflow velocity.
2. Δp_1 and Δp_2 will be kept constant at 540 mb and 340 mb respectively.
3. W_{p1} and W_{p2} for any particular dewpoint will be determined from figure 3 since Δp_1 and Δp_2 are known.
4. The value of Y is a function of the wind direction.

32. However, preliminary computations for several storms revealed that prior to the beginning of excessive precipitation, and between extended periods of precipitation when drier air moves into the area temporarily,

the assumption of saturation throughout the inflow and outflow layers does not hold. An examination of the Los Angeles storms disclosed that in no case did any appreciable precipitation occur when the dewpoints were lower than 40°F, and that the column of air could not be assumed to be saturated throughout its vertical extent until the surface dewpoint reached 65°F. It was necessary then to obtain some relationship between the amount of moisture that would be precipitated in a lifting process from a saturated column of air with a given surface dewpoint, and that which would occur when the column was not completely saturated. An analysis of this factor during observed rains showed that the relationship shown in figure 7 was a good approximation and could be used for dewpoints within the range of 40 to 65°F. Equation 2 then becomes

$$R = \left[f(T_D) \right] \left[\frac{V_1 \left(W_{p_1} - \frac{\Delta p_1}{\Delta p_2} W_{p_2} \right)}{Y} \right]$$

and rearranging,

$$R = V_1 \left[\frac{f(T_D) \left(W_{p_1} - \frac{\Delta p_1}{\Delta p_2} W_{p_2} \right)}{Y} \right] \qquad (4)$$

where $f(T_D)$ can be numerically evaluated from figure 7.

33. Before equation 4 was used for computing the maximum possible rainfall by increasing the variables to theoretical upper limits, its validity was tested in five of the major storms by inserting the observed or computed values of wind, dewpoint, etc. into the equation. To facilitate the computations it was possible to express most of equation 4 in graphic form, since $\frac{\Delta p_1}{\Delta p_2}$ was a constant, $f(T_D)$, W_{p_1} and W_{p_2} unique for any particular dewpoint, and Y a function of the wind direction. Figure 8 shows the graph in final form; the abscissa is $\frac{1}{Y}$ in terms of wind

direction, and the ordinate is

$$f(T_D)\ (W_{p_1} - \frac{\Delta p_1}{\Delta p_2}\ W_{p_2})$$

34. The value obtained from figure 8, Rainfall Computation Chart, is in inches per hour per unit wind velocity (mph) so that multiplying by the three-hourly geostrophic wind movement obtained from the three-hourly pressure maps yields the average depth of rainfall over 10,000 square miles for that period. When rainfall was not occurring over the entire area, this value was multiplied by the appropriate percentage.

35. The validity of equation 4 was demonstrated by applying it to storms chosen for their marked variation in rainfall intensity and duration. The January 1943 storm is the maximum storm of record over the area and the highest winds of record occurred in this storm and in the January 1916 storm. Furthermore, the storms of January 1916, February 1937, and February-March 1938 were selected because the extreme irregularity of their mass curves of rainfall would provide a rigorous test of the method of mass-curve reproduction. The storm of December 1933-January 1934 was included since its mass-curve characteristics were similar to the January 1943 storm, even though the rainfall duration and intensity were appreciably less than in the 1943 storm.

36. A synthetic construction of the mass curves for these storms was made and the results are shown in figure 9. The remarkable agreement of the mass curves theoretically computed for the five storms with the mass curves of average observed rainfall for the same storms demonstrates the validity of the equation. Tables 1 to 5 show the values of dewpoint, wind, rainfall, and other factors obtained from actual records and maps, and the 3-hourly average depths computed from equation 4.

37. Computations of correlation coefficients between the computed and observed amounts for 6 hours, 12 hours, and total-storm durations were made for all five storms to verify these relationships. The coefficients were 0.92 for 6 hours, 0.96 for 12 hours, and 0.99 for total storm.

Computation of the Maximum Possible Storm

38. With the relationships among the rain-producing factors established and verified quantitatively as outlined above, evaluation of these factors through time was necessary in order to compute the maximum possible storm. Since the complete arrangement of elements comprising a major meteorological event cannot be rationally synthesized, it was necessary to base the maximum possible storm on a known arrangement of the elements. The base from which the maximum possible storm was developed was the storm of January 1943, which not only produced the highest wind and greatest rainfall of record, but also outranked all others when theoretical rainfall was computed by increasing its winds and dewpoints to their physical upper limits. A 10% increase of wind movement over the 1943 storm value was incorporated into the computations. A greater increase in wind speed could not be justified by either direct or indirect aerological reckonings (see paragraph 9). The dewpoints possible in the maximum storm were determined from enveloping maximum dewpoint-duration curves, figure 10, for the coastal region of southern California and the dewpoint-duration curve of the January 1943 storm. Since, during a storm situation, high dewpoints do not persist for so long a period as indicated by the maximum curves, the enveloping data were given a rate of decrease approximating the rate observed in the 1943 storm.

39. Briefly, the steps taken were as follows:

1. Maximum dewpoints were tabulated for durations of

3 to 66 hours.

2. Three-hour wind movements during the 1943 storm were increased by 10% and tabulated.

3. These dewpoints and wind movements were grouped and arranged in the same chronologic order in which their relative magnitudes had been observed in 1943. In other words, the maximum 3-hour dewpoint and wind movement were placed in the same position in the storm sequence as the highest observed 3-hour dewpoint and wind movement.

4. The mean 3-hour wind-direction sequence experienced in the 1943 storm was maintained in the synthetic storm.

5. Three-hour values of precipitation were obtained by using the rainfall-computation chart, figure 8.

These values are presented in table 6.

40. In general, the rainfall of the maximum general storm, as well as the rainfall in the observed general storms, can be classified as stable orographic precipitation. This conclusion can be drawn because the basic hypothesis of a stable air mass flowing over a mountain barrier has satisfactorily accounted for the average depths over 10,000 square miles in the major storms. However, since the average depths over smaller areas have been greater, it is apparent that the same hypothesis cannot be extended, without modification, to the rainfall computation for smaller areas. Localized convergence, caused both by the storm dynamics and by the terrain, is added to the general orographic effect, increasing the local precipitation rates. For the purpose of better defining these local intensifications, and on the advice of Dr.

J. Bjerknes during his stay at this office, the computation for smaller areas was attempted.

41. Because it was the maximum-type storm and because of the greater number of gages operating in it, the January 1943 storm was selected as the test storm. Rectangles were fitted to five areas of maximum rainfall ranging from 200 to 5000 square miles on the total isohyetal map. The average height of the outflow barriers was found for each area for each mean 6-hour wind direction observed. Six-hour isohyetal maps were drawn for the entire Los Angeles area and all computations were made for 6-hour periods. Because of the variation in barrier height with wind direction and the fact that the Y used for 10,000 square miles was no longer applicable, it was not possible to use figure 8 in solving equation 4. A separate evaluation was made for each area during the storm period by using 6-hour wind movements, mean dewpoints, and mean wind directions from table 5 and the appropriate $f(T_D)$ from figure 7. By using the mean 6-hour dewpoints, Δp_2 and W_{p_2} could be obtained from figure 3 since they were unique for each given outflow barrier and wind direction. Since Δp_1 was held constant at 540 mb, W_{p_1} varied only with the dewpoint. However, there was no satisfactory way to determine the value of Y, the distance, parallel to the wind flow, over which the precipitation falls. Several complete computations were made, evaluating Y differently in each series, as for example, the distance from the coast to the barrier or the distance from the coast to the leeward limit of the area of appreciable precipitation. Consistent agreement between the computed and the observed precipitation was not obtained, and none of the methods of obtaining Y seemed to be substantially superior to any other.

42. Another series of computations was carried out after a rough separation of orographic from convergence precipitation. Theoretically, it was only the orographic rainfall which could be computed from equation 4 since the air flow implied was similar to that used for the 10,000-square-mile area (see figure 2). By inspection of the 6-hour isohyetal maps of the rainfall over the coastal regions farthest removed from the mountains, an amount was determined which was called the "base rainfall", or the rainfall during the 6-hour period which could be assumed to be due to convergence within the air mass itself and independent of the lift of the mountain barriers. This "base rainfall" was subtracted from the observed values. A new computation was made with Y measured as the mean distance from the "base rainfall" isohyet in the coastal region to the same isohyet in the lee of the mountains. To obtain comparable "observed" values this "base rainfall" was subtracted from the values actually observed. The results again were not sufficiently satisfactory to be used as the basis of an upward extrapolation of the observed parameters to their maximum possible values.

43. Various modifications of the above computation procedures were tested, including assumptions of air flow different from that shown in figure 2. No single flow model was sufficiently sensitive to the observable factors to produce increments of precipitation approximating those observed throughout the storm period. Rather, the use of several flow models or a varying model was indicated. A search was made for some characteristic of the storm, e.g., the distance of the Low center from the Los Angeles area, with which a systematic and consistent transition from one type of flow to another could be synchronized. No such phenomenon showed a correlation with the observed rainfall great enough to be used successfully.

44. The failure of the computation methods tested to reproduce the small-area rainfall must be charged to a combination of factors. The use of the same inflow-wind velocity for small areas as for 10,000 square miles was probably erroneous but the observations available did not permit a more detailed distribution across the area. It is also possible that the dewpoints used, representative for the 10,000-square-mile area, might need reexamination, although it is believed that any such error could not be of major importance. Omission of quantitative calculations of localized convergence effects is a recognized deficiency; that problem cannot be satisfactorily solved until adequate three-dimensional meteorological observations are available during storm periods.

45. Since the direct application of equation 4 to areas less than 10,000 square miles proved unsuccessful, an empirically modified method was finally adopted. Instead of adjusting rainfall values reproduced by theoretical means, the observed rainfall values were adjusted - those observed rainfall values containing in themselves a measure of the localized convergence and convective effects otherwise unevaluated. Essentially the method is the same as that used for the 10,000-square-mile computation. It also involves an increase of the observed moisture and wind values of the January 1943 storm to the maximum possible. Mean mass curves for the maximum point, 25, 50, 100, 250, 500, 1000, 2500, and 5000-square-mile areas were drawn and the observed dewpoint-duration curve was plotted by mean 6-hour increments. Using the observed mean 6-hour wind directions, the mean 6-hour values of W_{LA}, were tabulated. A corresponding tabulation of W_{LA}, using the maximum possible dewpoints, was made. The ratios of the maximum W_{LA} values to the observed values were computed as percentages and then multiplied by 110% to allow for the increased

wind movement in the maximum storm. By applying these increases to the observed 6-hour precipitation increments over the various areas, the maximum mass curves were obtained and the resulting depth-area data plotted and enveloped in figure 11. The values for the 1-hour and 3-hour durations were obtained by utilizing the maximum 1-hour and 3-hour data in a similar manner.

46. While figure 11 gives the depth-area data for the maximum general storm, it is recognized that for small areas and short durations, these values can be and, in fact, have been exceeded. This calls for the determination of the maximum "local" storm which can occur over the Los Angeles area. It is certain that the maximum local rainfall will be experienced within a fairly general storm situation, but not during the maximum general storm. Salient meteorological features of the latter storm preclude such an event. Most obvious of all is the fact that the extreme wind velocities of the maximum storm will not permit the convective activity to great heights which is apparently necessary for maximum local rainfall. The January 1943 storm illustrated this point, since no thunderstorm activity was reported until the major portion of the precipitation was over.

Maximum Local Storms

47. The type of storm which produces the highest rainfall intensities for short durations over small areas is the thunderstorm. The thunderstorm's characteristic cumulonimbus cloud illustrates the type of flow essentially responsible for its formation - convergent radial inflow at the bottom and divergent radial outflow at the top. Other types of flow such as translation - of greater magnitude and better observed - are often superimposed on the basic flow. The air ascends at vertical velocities dependent

on the magnitude and depth of radial inflow and on the internal properties of the air mass rather than on cyclonic activity or topography, although the latter often provide the initial impulses to thunderstorm formation. Available analyses of rainfall indicate that, except for extremely short and therefore negligible durations, the same maximum vertical velocities (and resulting raindrop concentrations) can occur anywhere in the United States. The possible volume of rainfall produced in the maximum case thus becomes a function of the moisture content of the air mass processed.

48. In earlier reports of the Hydrometeorological Section, particularly Nos. 2 and 3 for the Ohio River Basin above Pittsburgh and for the Sacramento Basin, respectively, a radial-inflow model of the type discussed was used for the computation of the effective precipitable water W_E as a function of dewpoint at 1000 mb. Further investigations have disclosed weaknesses in that model - most important being (1) a violation of continuity of mass flow and (2) a variation of cell height (and therefore also a variation of depth of convergent layer) inconsistent with observations of cumulonimbus heights. To correct these weaknesses a series of models, all containing the following features, have been studied:

(1) Continuity of mass flow, by allowing equal mass (equal vertical pressure differences) in convergent and divergent layers or by correcting any inequality by adjustment of outflow velocity by the ratio of inflow Δp to outflow Δp.

(2) Variation of total cell height linearly with surface vapor pressure (a function of dewpoint at constant pressure) from 300 mb at a 1000-mb dewpoint of 50°F to 100 mb at a 1000-mb dewpoint of 78°F.

The depth of the convergent layer was varied from one third to two thirds of the pressure height of the total cell; the divergent layer from one

third to one half of the same height; and the middle layer from one third of the height to zero. Each of these models produced a different value of W_E for a specific dewpoint but the percentage variation of W_E with dewpoint in all models was very nearly the same as the variation of W_p with dewpoint, W_p being computed from 1000 mb to the top of the cell. This fact allows for a moisture adjustment of thunderstorm rainfall without reference to the particular flow model or to a specific value of W_E. Even the rainfall resulting from a group of thunderstorms rather than one can be dealt with in the same fashion. Since in the maximum thunderstorm situation it is assumed that the maximum dynamics have been achieved, the ratio of maximum possible thunderstorm-rainfall intensities over two regions at the same elevation is equal to the ratio of their maximum possible W_p values, defined above.

49. The upper limits of thunderstorm rainfall are reasonably well defined by an envelopment of maximum rainfall observed in the United States over small areas and for short durations. The dewpoints in these storms equal or approach the maximum possible and the dynamic intensities may also be assumed to be the maximum. To estimate the limiting thunderstorm-rainfall rates over specific regions it is thus necessary only to compare the possible surface dewpoints and to multiply the enveloping rates by the ratio of the corresponding W_p's. The maximum local-storm depth-area values were derived in this fashion and are given in figure 12. For the enveloping values the one-hour dewpoint is 78°F (considered to be the maximum possible in a rain situation anywhere in the United States) and for the Los Angeles area the maximum possible dewpoint is 67°F. The percentage of the one-hour enveloping rate possible over the Los Angeles area is, on this basis, 58. For other durations, the corresponding variations of the dewpoints with time were considered.

50. The local-storm values of figure 12 are for the season November through April. They exceed the maximum general-storm values only for durations under 12 hours and the areas indicated in the figure. For the smallest areas and shortest durations they themselves may be exceeded by the local storm occurring in the summer because of the higher dewpoints that can occur in that season. The rainfall of August 12, 1891, at Campo is a case in point. This occurred at a dewpoint of 72°F, which is also the annual maximum possible in the region. Adjusting the envelopping U. S. values downward to this dewpoint gives a value of 8.5 inches in one hour over one square mile, a good agreement with the observed point value of 11.5 inches in 80 minutes at Campo. However, the meteorological situation peculiar to the West Coast in the summer limits the effectiveness of the rainfall process. Although not accurately definable in a quantitative way, it is the opinion of the Hydrometeorological Section that the summer thunderstorm in the Los Angeles area, whose maximum one-hour value over one square mile is given above, will rapidly taper down so that for an area of 50 square miles and a duration of two hours it will no more than equal the corresponding winter-storm local rainfall values. For larger areas and longer durations, the winter local storm will produce greater depths.

51. The local-storm values of figure 12 are for occurrences at sea level. There is no orographic intensification of the limiting thunderstorm rate, but there is an orographic depleting effect. The higher the level at which the storm occurs, the less the total W_p that can be processed and the less the rainfall. A study of all the radial-inflow models previously described also showed that in all cases the depleting effect, expressed as a percentage, approximately equaled the ratio of the W_p

computed from the barrier elevation to the top of the cell to the W_p computed from 1000 mb to the top of the cell. The percentages of the limiting rainfall rate at sea level that are possible at higher elevations, for 1000-mb dewpoints around 67°F are given below:

Elevation (ft.)	500	1000	1500	2000	2500	3000	4000	5000	6000	7000	8000
%	95	91	87	83	79	75	68	61	54	48	43

These percentages are applicable to all areas and durations of the local storm.

Distribution of Maximum Possible Rainfall

52. Because of its critical nature for small basins with short concentration times, some indication of the time breakdown of maximum local rainfall for durations less than one hour is necessary. The only available data for such durations is from point-rainfall observations. The Hydrometeorological Section has in process a compilation of the maximum recorded intensities at first-order Weather Bureau stations for 5, 10, 15, 30 and 60 minutes. A study of these values shows a significant variation of the percentage depth-duration curves with change of the one-hour amount, such that the percentage of the one-hour amount that can fall in the shorter period decreases with increase of the one-hour amount. The magnitude of the decrease also decreases with increase of the one-hour amount, so that a limiting percentage depth-duration curve applicable to maximum possible intensities can be reliably estimated. This has been done and the percentages applied (with some smoothing) to the maximum depths for one square mile. They cannot be applied without modification to larger areas. An analysis of percentage depth-duration data for periods greater than one hour indicates a variation of the relationship such that the partial-duration percentage depths decrease with increasing area. An extrapolation of this indicated variation with area has been tied in with the percentage

depth-duration values for one square mile to give the 15-minute curves of figure 12 up to 250 square miles.

53. The possible geographical location of the maximum local storm and also the geographical distribution of the rainfall within the maximum general storm cannot be fully defined from the data available at this time. A distribution based on the mean seasonal isohyetal pattern is serviceable but only within limits, since the pattern is the summation of a variety of storm occurrences, most of which are far from the maximum possible. The mean seasonal pattern is influenced more by frequency of occurrence than by magnitude of occurrence while the maximum possible has, naturally, an extremely low frequency.

54. For the geographical distribution within the maximum general storm, the Hydrometeorological Section suggests that the best guide is the distribution within the January 1943 storm. This storm is closest to the maximum general storm and has, in fact, served as the basis for its computation. Not only are wind speeds and dewpoints the highest recorded in such storms; the wind directions - a determining factor influencing the distribution - are the most critical.

55. For example, to determine the maximum average depth in the maximum general storm over a project 100-square-mile area, the January 1943 storm is used as the basic pattern of intensity distribution in the following way: The ratio of the 100-square-mile depth in figure 11 to the maximum 100-square-mile depth in the January 1943 storm is computed. The January 1943 depth over the project area is then multiplied by the computed ratio and the result is the maximum average depth over the project area in the maximum possible general storm.

56. The maximum local storm is a different problem. It is not as well controlled by topography as the general storm, although topography plays an equally important part in influencing frequency of local-storm occurrence. The general storm, for instance, is the feature of the middle of the rainy season - December and January - while the local storm characterizes the beginning and ending of the season. The significance of this is borne out by a statistical study not yet completed by the Hydrometeorological Section which shows that the correlation between elevation and mean monthly rainfall is highest in January and lowest in November and April.

57. The high wind velocities of the maximum general storm prevent the extreme convective effects necessary for the maximum local storm and spread the resulting rainfall over larger areas. The maximum local storm is more likely to occur with low wind velocities, if the convergence effects are present. Even on the coastal plain, this fact means that the usual stabilizing effects of the low ocean temperatures need not be present over the small areas and for the short durations of the maximum local storm. The conclusion, therefore, is that the maximum local storm can occur anywhere in the Los Angeles area and that its rainfall is reduced rather than increased by elevation. The table of paragraph 51 gives the proper percentage adjustments to be used at various elevations. For basins extending over a range of elevations, the mean elevation should be used in entering this table.

58. The areal distribution of intensities within the maximum local storm cannot be defined accurately. For that reason, it is suggested that the most critical hydrologic distribution be used. The only restriction

in any isohyetal pattern so constructed is that the average depth over the sub-areas encompassed by specific isohyets, or between specific isohyets, should not exceed the depths of figure 12 after these depths are reduced to the mean elevation of the sub-areas concerned.

Table 1

Rainfall Computations

Storm of January 24-28, 1916

Date	Period	Wind Direction	Dew Point	# W_{LA}	* %	V_{geos}	ΔR	Accumulated R Computed	Accumulated R Observed
1/24	12-15	239	51	.00250	30	50	.037	.	
	15-18	234	52	.00292	35	56	.057	.09	0.1
	18-21	254	53	.00258	60	59	.091		
	21-24	256	53	.00250	60	63	.094	.28	0.1
1/25	00-03	257	52	.00220	75	83	.137		
	03-06	264	52	.00191	75	72	.103	.52	0.4
	06-09	280	52	.00113	75	107	.091		
	09-12	280	53	.00127	50	132	.084	.69	0.6
	12-15	281	53	.00127	45	155	.089		
	15-18	300	53	.00127	60	194	.148	.93	0.7
	18-21	300	52	.00113	60	216	.146		
	21-24	301	51	.00103	60	196	.121	1.20	0.9
1/26	00-03	303	50	.00091	45	175	.072		
	03-06	298	49	.00078	30	174	.041	1.31	1.0
	06-09	300+	-	-	-	-	.000		
	09-12	300+	-	-	-	-	.000	1.31	1.0
	12-15	300+	-	-	-	-	.000		
	15-18	300+	-	-	-	-	.000	1.31	1.0
	18-21	276	50	.00106	100	52	.055		
	21-24	234	51	.00257	100	86	.221	1.59	1.3
1/27	00-03	222	52	.00311	100	122	.380		
	03-06	225	53	.00342	100	125	.428	2.40	2.4
	06-09	237	55	.00390	100	151	.590		
	09-12	230	56	.00440	100	188	.827	3.81	3.8
	12-15	260	56	.00306	100	269	.824		
	15-18	267	56	.00260	100	250	.650	5.29	4.8
	18-21	280	54	.00139	70	274	.267		
	21-24	292	51	.00103	30	267	.082	5.64	5.2
1/28	00-03	300+	-	-	-	-	.000		
	03-06	300+	-	-	-	-	.000	5.64	5.5

* Percent of area south of front or trough line or percent of area experiencing upslope winds based on isobaric pattern.

$$\# \; W_{LA} = \frac{f(T_D) \left(W_{P1} - \frac{540}{340} W_{P2} \right)}{Y}$$

taken from figure 8, Rainfall Computation Chart.

Table 2

Rainfall Computations

Storm of December 30, 1933-January 1, 1934

Date	Period	Wind Direction	Dew Point	# W_{LA}	* %	V_{geos}	ΔR	Accumulated R Computed	Accumulated R Observed
12/30	12-15	230	56	.00441	90	53	.211		
	15-18	236	54	.00352	90	47	.149	.36	0.3
	18-21	235	55	.00389	100	65	.252		
	21-24	235	55	.00389	100	61	.237	.85	0.6
12/31	00-03	223	55	.00417	100	70	.282		
	03-06	215	56	.00465	100	84	.391	1.52	1.0
	06-09	192	55	.00404	100	108	.436		
	09-12	192	56	.00440	100	115	.505	2.46	1.9
	12-15	206	56	.00464	100	147	.681		
	15-18	214	55	.00426	100	138	.578	3.72	3.3
	18-21	215	56	.00465	100	164	.763		
	21-24	236	56	.00423	100	139	.588	5.07	4.4
1/1	00-03	220	56	.00461	100	101	.466		
	03-06	218	56	.00463	100	88	.407	5.84	5.4
	06-09	249	56	.00368	100	87	.320		
	09-12	240	57	.00439	100	81	.355	6.62	6.2
	12-15	241	58	.00465	100	67	.312		
	15-18	197	55	.00414	50	49	.101	7.03	6.4
	18-21	183	55	.00378	15	22	.012		
	21-24	18	-	-	-	-	.000	7.04	6.5

* Percent of area south of front or trough line or percent of area experiencing upslope winds based on isobaric pattern.

$$\# W_{LA} = \frac{f(T_D)\ \left(W_{P1} - \frac{540}{340}\ W_{F2}\right)}{Y}$$

taken from figure 8, Rainfall Computation Chart

Table 3

Rainfall Computations

Storm of February 13-14, 1937

Date	Period	Wind Direction	Dew Point	# W_{LA}	* %	V_{geos}	ΔR	Accumulated R Computed	Accumulated R Observed
2/13	06-09	153	48	.00100	100	84	.084		
	09-12	165	52	.00218	100	96	.209	.29	0.2
	12-15	175	52	.00256	100	90	.230		
	15-18	195	53	.00340	100	94	.320	.84	0.7
	18-21	222	53	.00347	100	110	.382		
	21-24	216	53	.00352	100	145	.510	1.73	1.9
2/14	00-03	219	53	.00348	100	136	.474		
	03-06	242	52	.00271	100	126	.342	2.55	3.0

* Percent of area south of front or trough line or percent of area experiencing upslope winds based on isobaric pattern.

$$\# W_{LA} = \frac{f(T_D)\left(W_{P1} - \frac{540}{340} W_{P2}\right)}{Y}$$

taken from figure 8, Rainfall Computation Chart.

Table 4

Rainfall Computations

Storm of February 27-March 3, 1938

Date	Period	Wind Direction	Dew Point	# W_{LA}	* %	V_{geos}	ΔR	Accumulated R Computed	Accumulated R Observed
2/27	12-15	137	-	-	-	-	.000	-	-
	15-18	170	57	.00378	100	64	.242	.24	0.3
	18-21	182	57	.00436	100	75	.328		
	21-24	199	58	.00525	100	58	.304	.87	0.7
2/28	00-03	200	58	.00527	100	38	.200		
	03-06	200	58	.00527	100	45	.237	1.31	1.0
	06-09	209	58	.00536	100	59	.316		
	09-12	216	59	.00566	80	82	.372	2.00	1.4
	12-15	232	59	.00532	60	98	.313		
	15-18	221	59	.00558	65	112	.407	2.72	1.9
	18-21	234	58	.00495	100	98	.485		
	21-24	235	58	.00491	100	75	.368	3.57	3.4
3/1	00-03	235	56	.00427	100	45	.192		
	03-06	243	55	.00365	70	46	.118	3.88	3.8
	06-09	245	56	.00388	50	60	.116		
	09-12	248	57	.00402	75	42	.127	4.12	3.8
	12-15	243	57	.00426	60	55	.141		
	15-18	276	56	.00197	60	63	.074	4.34	3.8
	18-21	248	55	.00342	35	96	.115		
	21-24	254	56	.00341	50	120	.204	4.66	4.0
3/2	00-03	244	56	.00392	100	124	.486		
	03-06	224	57	.00492	100	126	.620	5.76	5.2
	06-09	220	60	.00591	100	138	.816		
	09-12	224	60	.00583	100	146	.851	7.43	7.1
	12-15	232	60	.00558	100	128	.715		
	15-18	238	58	.00478	100	146	.698	8.84	9.2
	18-21	253	57	.00374	100	117	.438		
	21-24	270	54	.00200	100	102	.204	9.49	9.8
3/3	00-03	269	54	.00206	100	99	.204		
	03-06	274	54	.00176	100	95	.167	9.86	10.2
	06-09	274	53	.00160	100	101	.162		
	09-12	277	50	.00102	100	104	.106	10.12	10.6

* Percent of area south of front or trough line or percent of area experiencing upslope winds based on isobaric pattern.

$$\# W_{LA} = \frac{f(T_D)\left(W_{P1} - \frac{540}{340} W_{P2}\right)}{Y}$$

taken from figure 8, Rainfall Computation Chart.

Table 5

Rainfall Computations

Storm of January 21-23, 1943

Date	Period	Wind Direction	Dew Point	# W_{LA}	* %	V_{geos}	ΔR	Accumulated R Computed	Accumulated R Observed
1/21	00-03	255	42	.00028	50	102	.014		
	03-06	253	44	.00062	50	137	.042	.06	0.1
	06-09	245	46	.00111	60	142	.094		
	09-12	240	48	.00164	55	160	.144	.29	0.5
	12-15	245	52	.00262	75	176	.346		
	15-18	243	53	.00298	100	203	.605	1.24	1.2
	18-21	245	55	.00375	100	202	.758		
	21-24	250	57	.00390	100	191	.745	2.75	2.5
1/22	00-03	255	57	.00364	100	165	.601		
	03-06	240	57	.00440	100	125	.550	3.90	4.0
	06-09	235	57	.00464	100	160	.743		
	09-12	230	57	.00476	100	160	.762	5.40	5.1
	12-15	230	57	.00476	100	180	.858		
	15-18	215	58	.00535	100	215	1.150	7.41	6.9
	18-21	235	58	.00491	100	272	1.336		
	21-24	238	58	.00478	100	221	1.058	9.81	9.0
1/23	00-03	240	57	.00440	100	167	.735		
	03-06	245	56	.00388	100	139	.539	11.08	10.4
	06-09	260	55	.00286	100	144	.412		
	09-12	262	56	.00293	100	149	.437	11.93	11.2
	12-15	265	55	.00253	100	119	.302		
	15-18	290	54	.00138	100	107	.148	12.38	11.7
	18-21	300	-	-	-	-	.000		
	21-24	305	-	-	-	-	.000	12.38	11.8

* Percent of area south of front or trough line or percent of area experiencing upslope winds based on isobaric pattern.

$$\# \; W_{LA} = \frac{f(T_D) \quad (W_{P1} - \frac{540}{340} \; W_{P2})}{Y}$$

taken from figure 8, Rainfall Computation Chart

Table 6

Rainfall Computations

Maximum Possible Storm

(Based on the chronological pattern of dewpoint and wind velocity in the January 1943 storm, dewpoints increased to maximum in accordance with the Enveloping Maximum Dewpoint-Duration Curve, wind speeds increased 10%, other factors kept constant.)

3-hr. Period	Wind Direction	Dew Point	# W_{LA}	* %	V geos	Δ R	Accumulated R
1	255	49.8	.00175	50	112	.10	.10
2	253	51.7	.00226	50	151	.17	.27
3	245	53.3	.00300	60	156	.28	.55
4	240	54.6	.00360	55	176	.35	.90
5	245	55.8	.00380	75	194	.55	1.45
6	243	56.8	.00418	100	223	.93	2.38
7	245	58.0	.00446	100	222	.99	3.37
8	250	58.7	.00432	100	210	.91	4.28
9	255	59.2	.00411	100	182	.75	5.03
10	240	59.5	.00509	100	138	.70	5.73
11	235	59.9	.00543	100	176	.95	6.68
12	230	60.3	.00574	100	176	1.01	7.69
13	230	60.9	.00590	100	198	1.17	8.86
14	215	62.4	.00663	100	236	1.56	10.42
15	235	63.8	.00636	100	299	1.90	12.32
16	238	61.5	.00573	100	243	1.39	13.71
17	240	59.0	.00496	100	184	.91	14.62
18	245	58.5	.00458	100	153	.70	15.32
19	260	58.4	.00360	100	158	.57	15.89
20	262	58.2	.00342	100	164	.56	16.45
21	265	58.1	.00316	100	131	.41	16.86
22	290	57.6	.00186	100	118	.22	17.08

* Percent of area south of front or trough line or percent of area experiencing upslope winds based on isobaric pattern.

$$\# \; W_{LA} = \frac{f(T_D) \quad (W_{P1} - \frac{540}{340} W_{P2})}{Y}$$

taken from figure 8, Rainfall Computation Chart.

COMPARATIVE INFLOW AND OUTFLOW VELOCITIES

FIGURE 1 - VERTICAL STRETCHING DUE TO DECELERATION

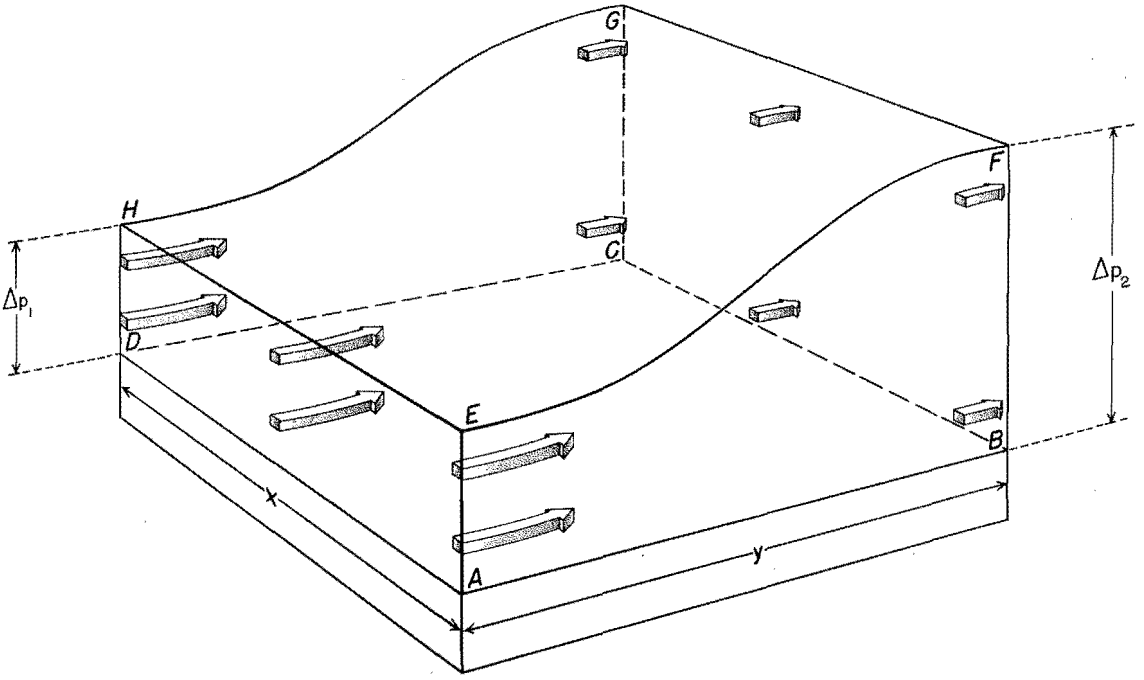

FIGURE 2 - FLOW OVER AN IDEALIZED BARRIER

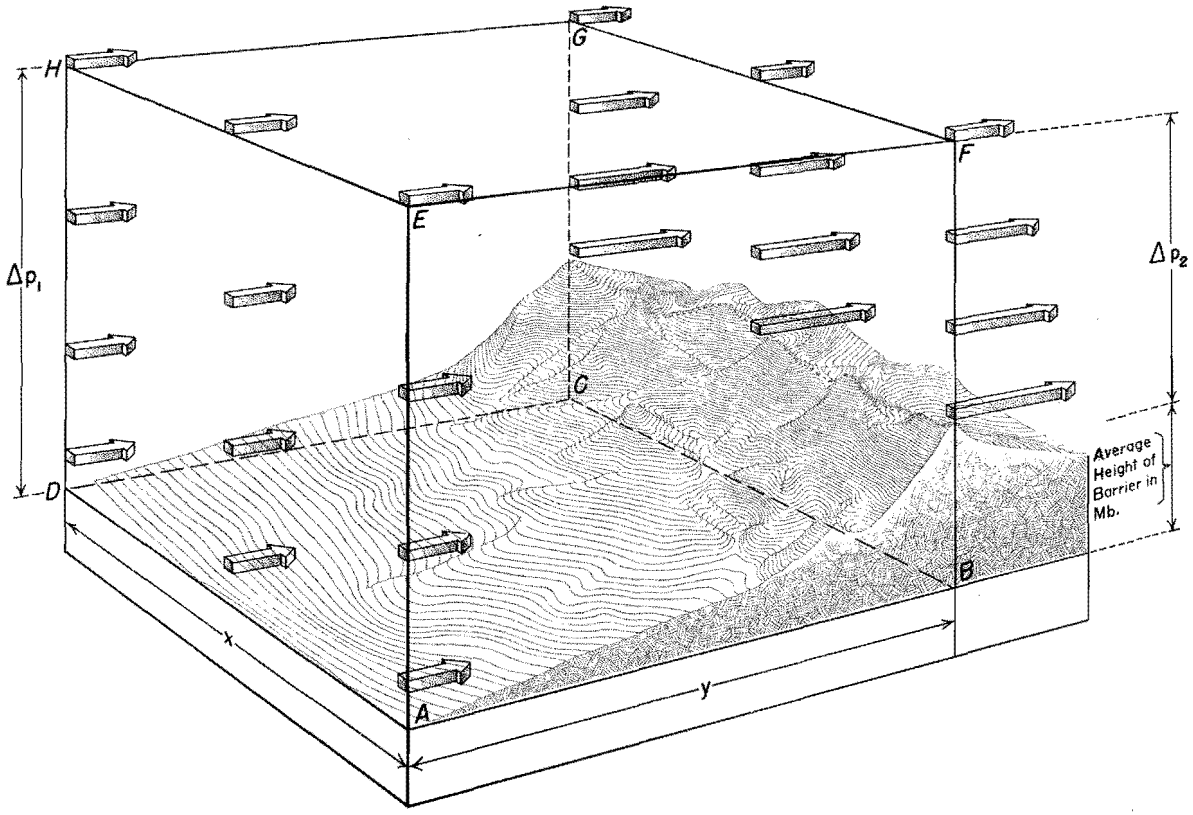

FILE 45001

DEPTHS OF PRECIPITABLE WATER IN A COLUMN OF AIR OF GIVEN HEIGHT ABOVE 1000 MILLIBARS

Assuming Saturation with a Pseudo-Adiabatic Lapse Rate for the Indicated Surface Temperatures

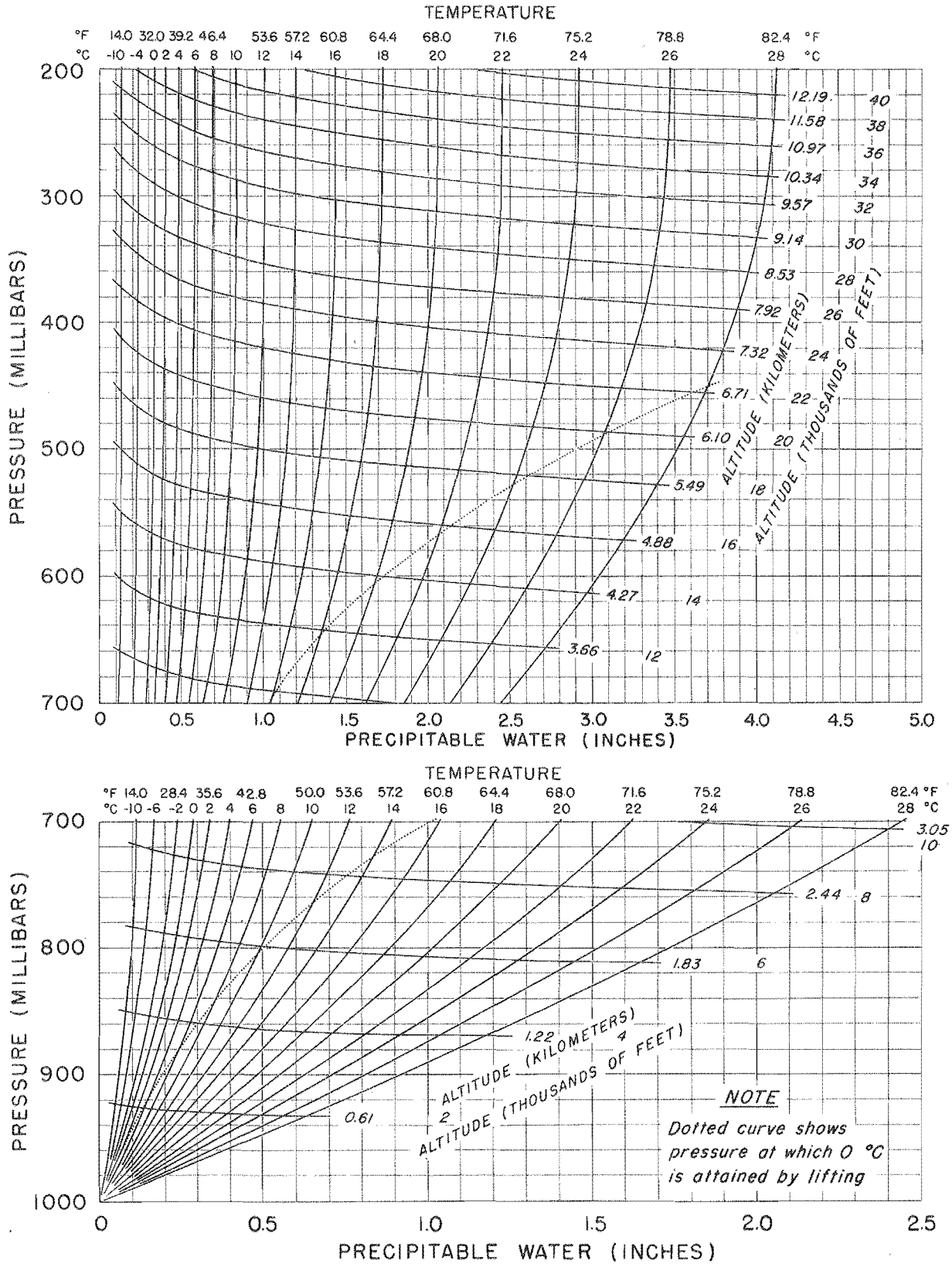

FILE 45007

FIGURE 3

COMPUTATION CHART FOR 10000-FOOT PRESSURES

(ASSUMING PSEUDO-ADIABATIC LAPSE RATE)

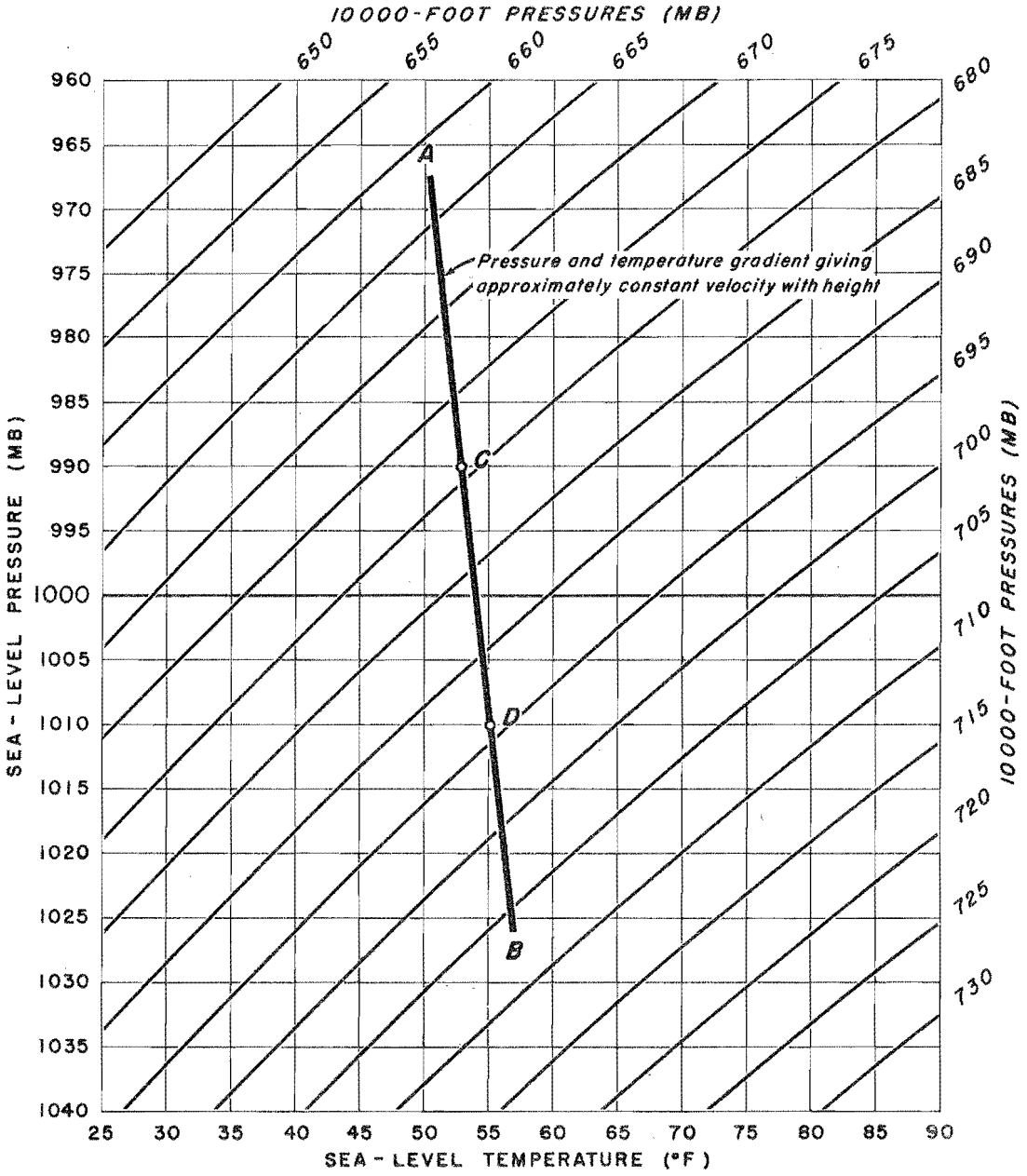

RELATIVE-HUMIDITY CORRECTION

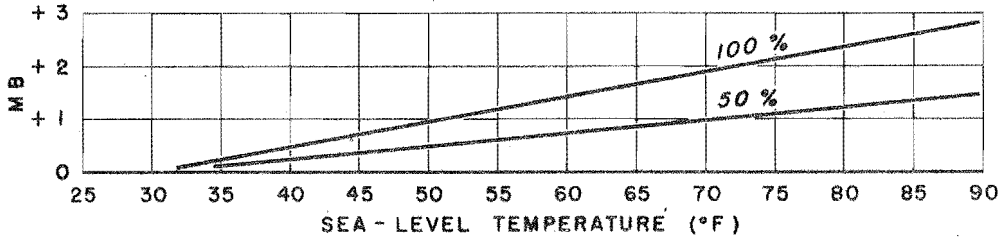

FILE 44135

FIGURE 4

VARIATION OF VELOCITY WITH HEIGHT FROM SEA-LEVEL TO 20000 FEET DURING TYPICAL STORM CONDITIONS OVER SOUTHERN CALIFORNIA

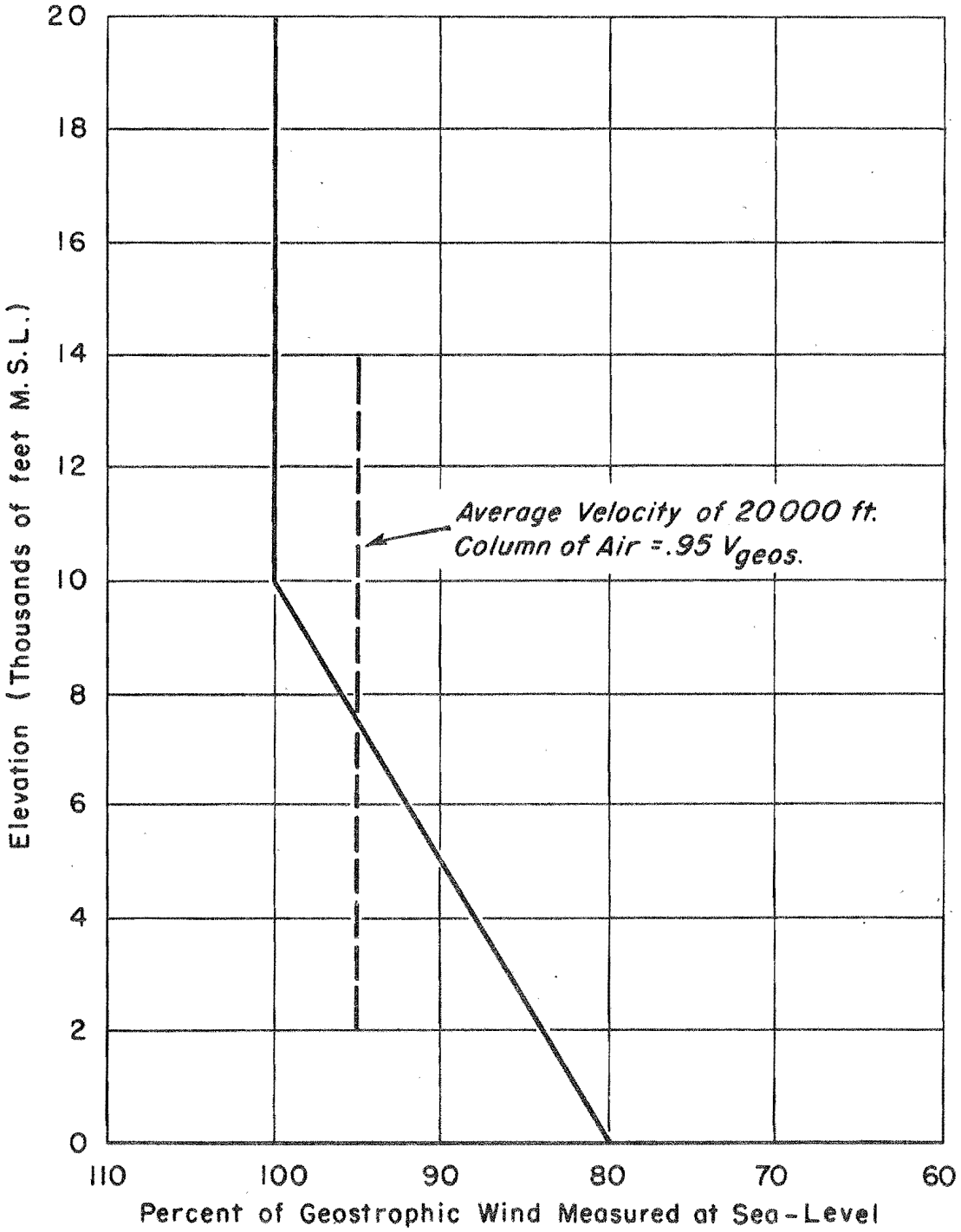

FILE 44133

FIGURE 5

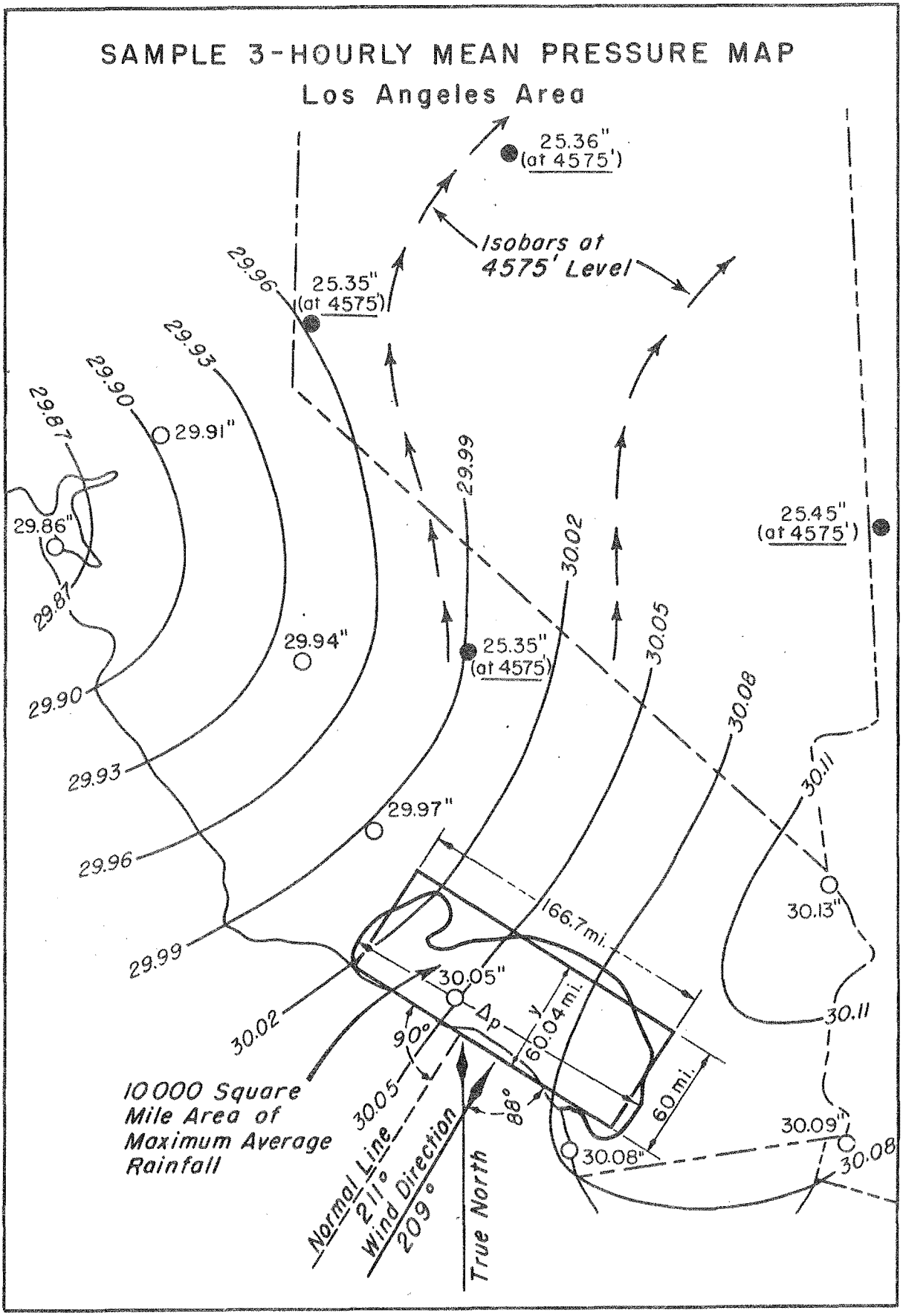

FILE 44134

FIGURE 6

RELATION OF REDUCED DEW POINT TO PERCENTAGE OF $(Wp_1 - \frac{\Delta p_1}{\Delta p_2} Wp_2)$

LOS ANGELES AREA

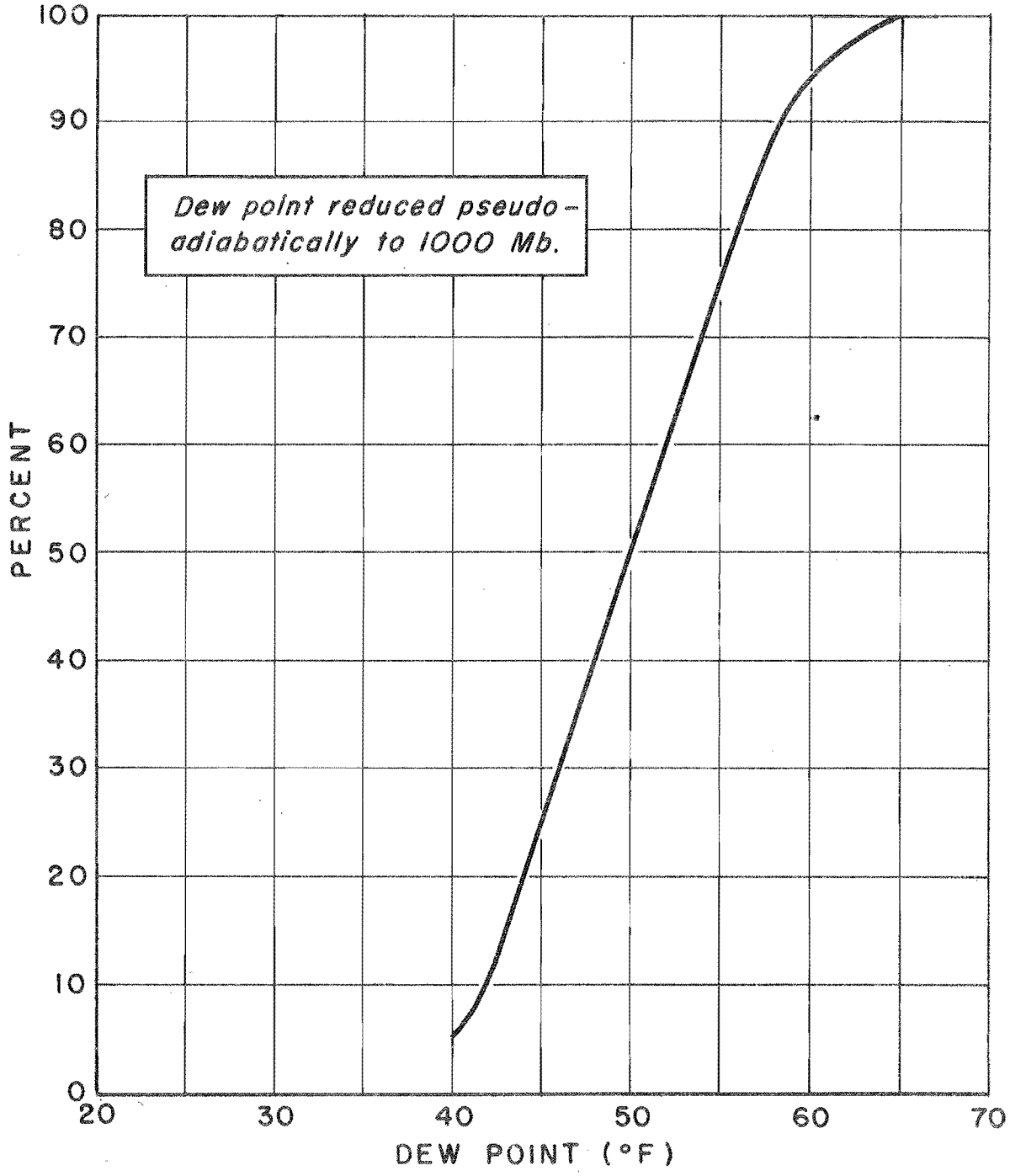

FILE 44125

FIGURE 7

RAINFALL COMPUTATION CHART FOR THE LOS ANGELES AREA

Maximum Average Rainfall Over 10000 Square Miles as a Function of Wind Direction and Reduced Dew Point

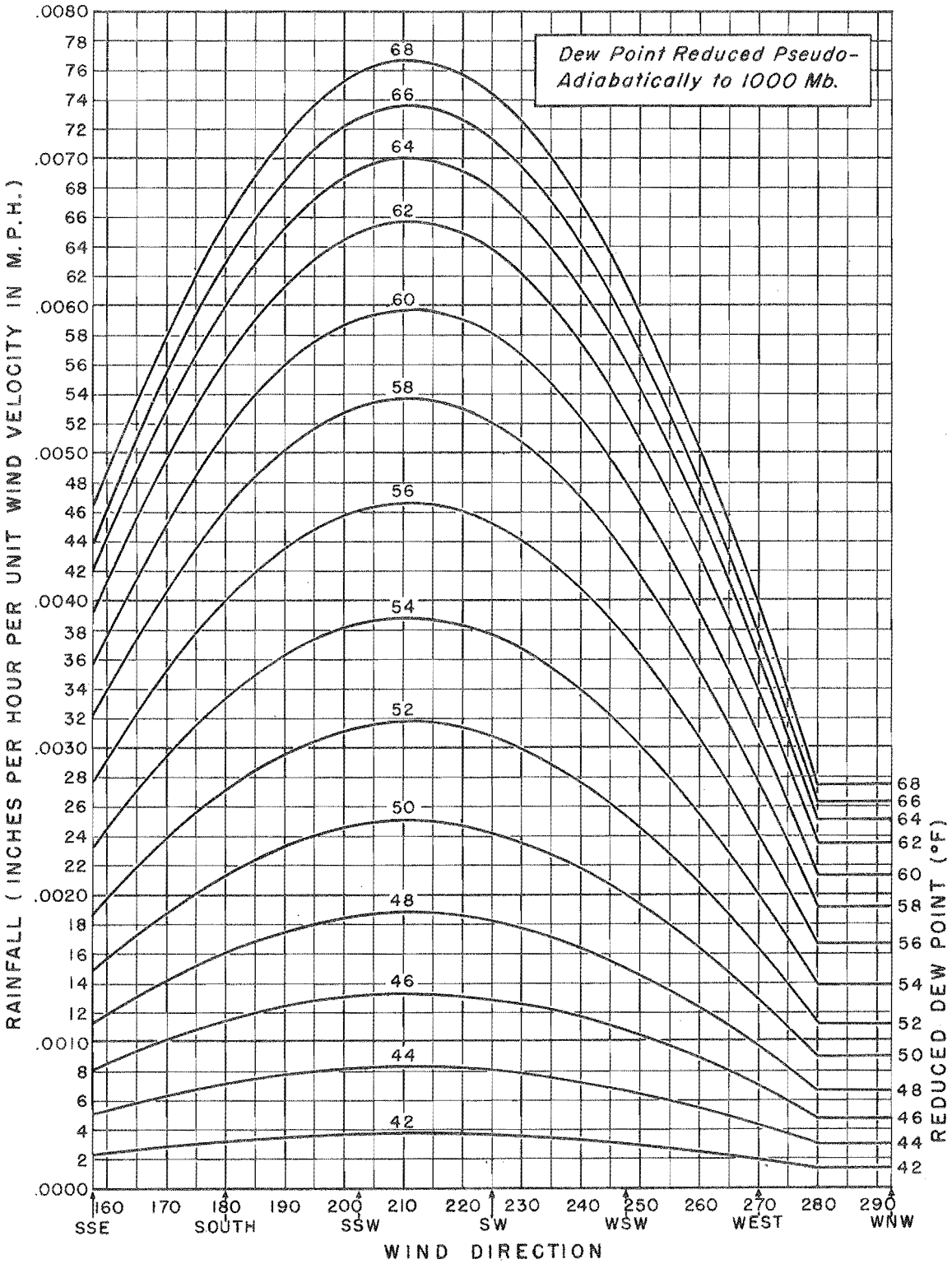

FILE 44126

FIGURE 8

U. S. DEPARTMENT OF COMMERCE
WEATHER BUREAU
HYDROMETEOROLOGICAL SECTION

MASS CURVES OF MAXIMUM AVERAGE RAINFALL OVER 10000 SQUARE MILES

BY STORM PERIODS OVER SOUTHERN CALIFORNIA

LEGEND

—— Observed

---- Computed

FIGURE 9

FILE 44124

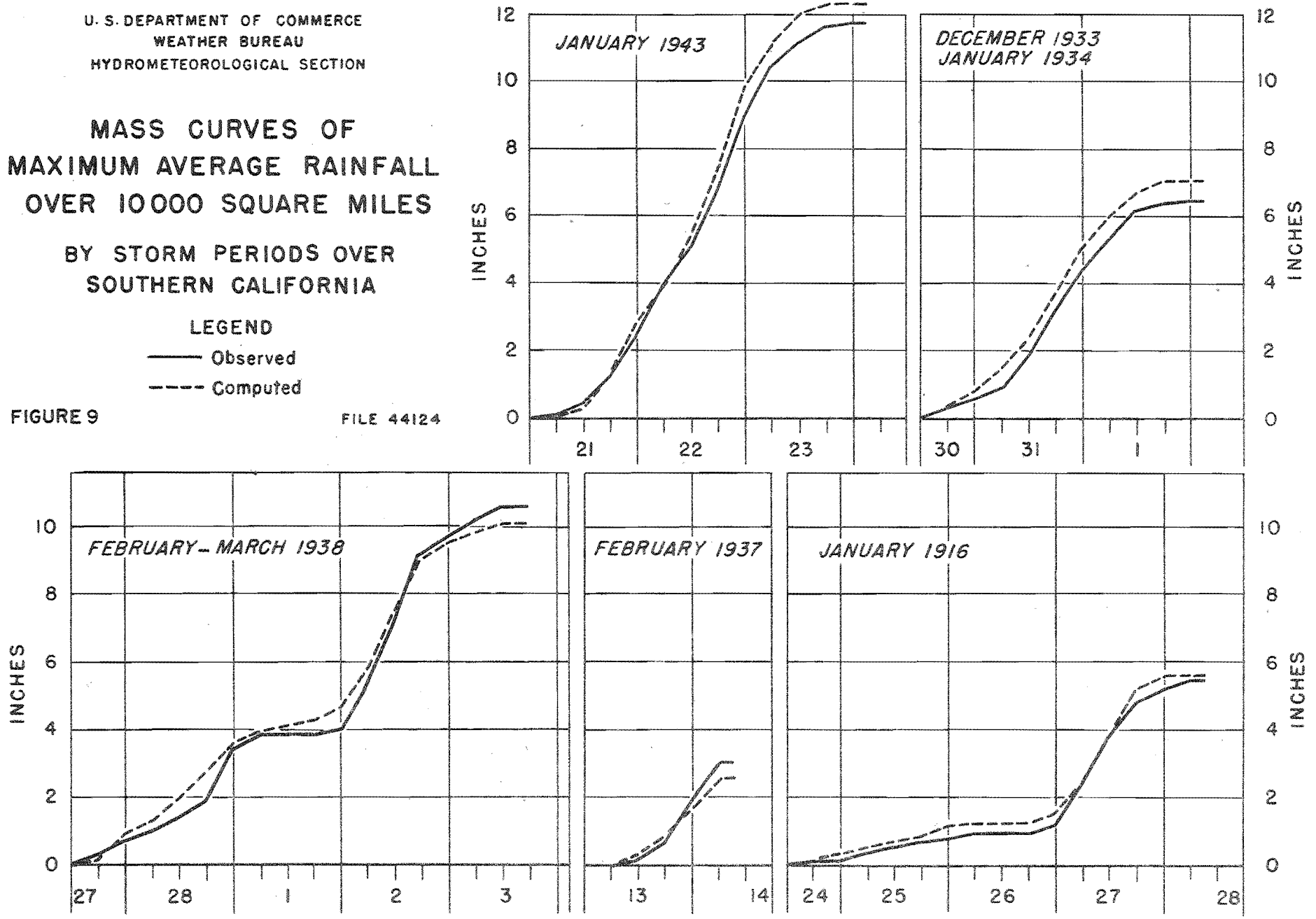

ENVELOPING MAXIMUM DEWPOINT-DURATION CURVES FOR THE COASTAL REGION OF SO. CALIFORNIA

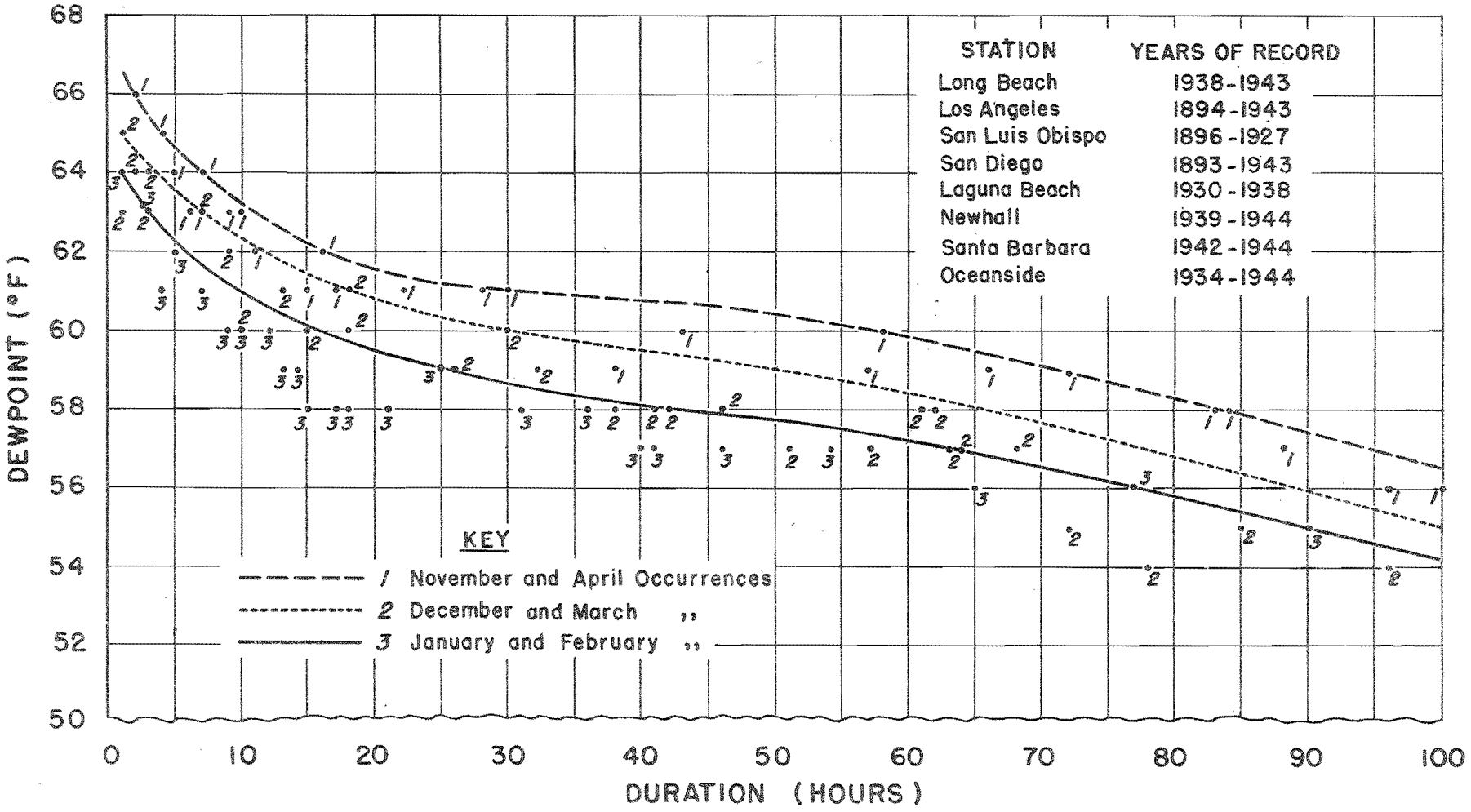

FIGURE 10

FILE 45043

DEPTH-AREA CURVES
MAXIMUM POSSIBLE GENERAL STORM
LOS ANGELES AREA

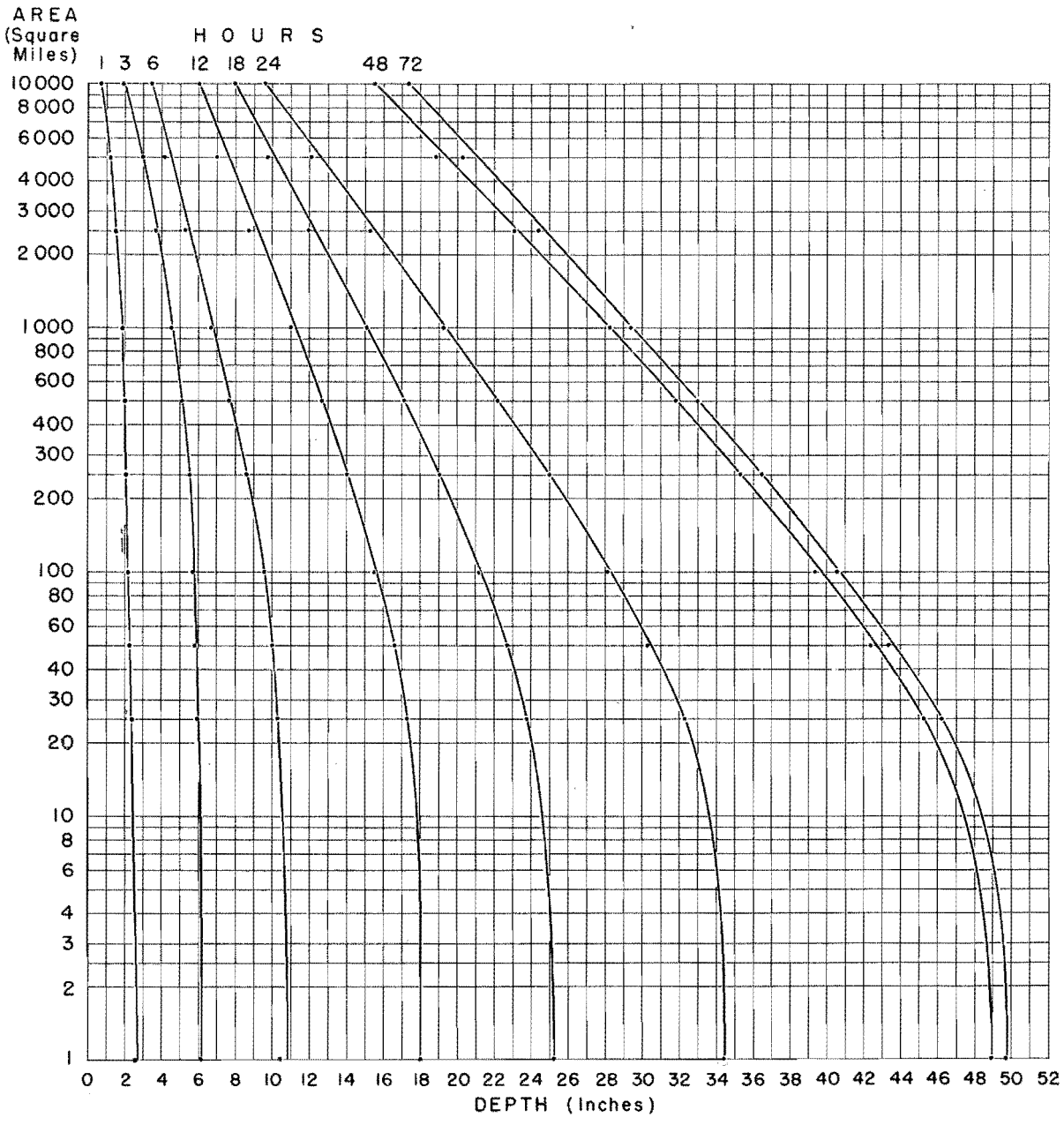

FIGURE 11

DEPTH-AREA CURVES MAXIMUM POSSIBLE LOCAL STORM LOS ANGELES AREA

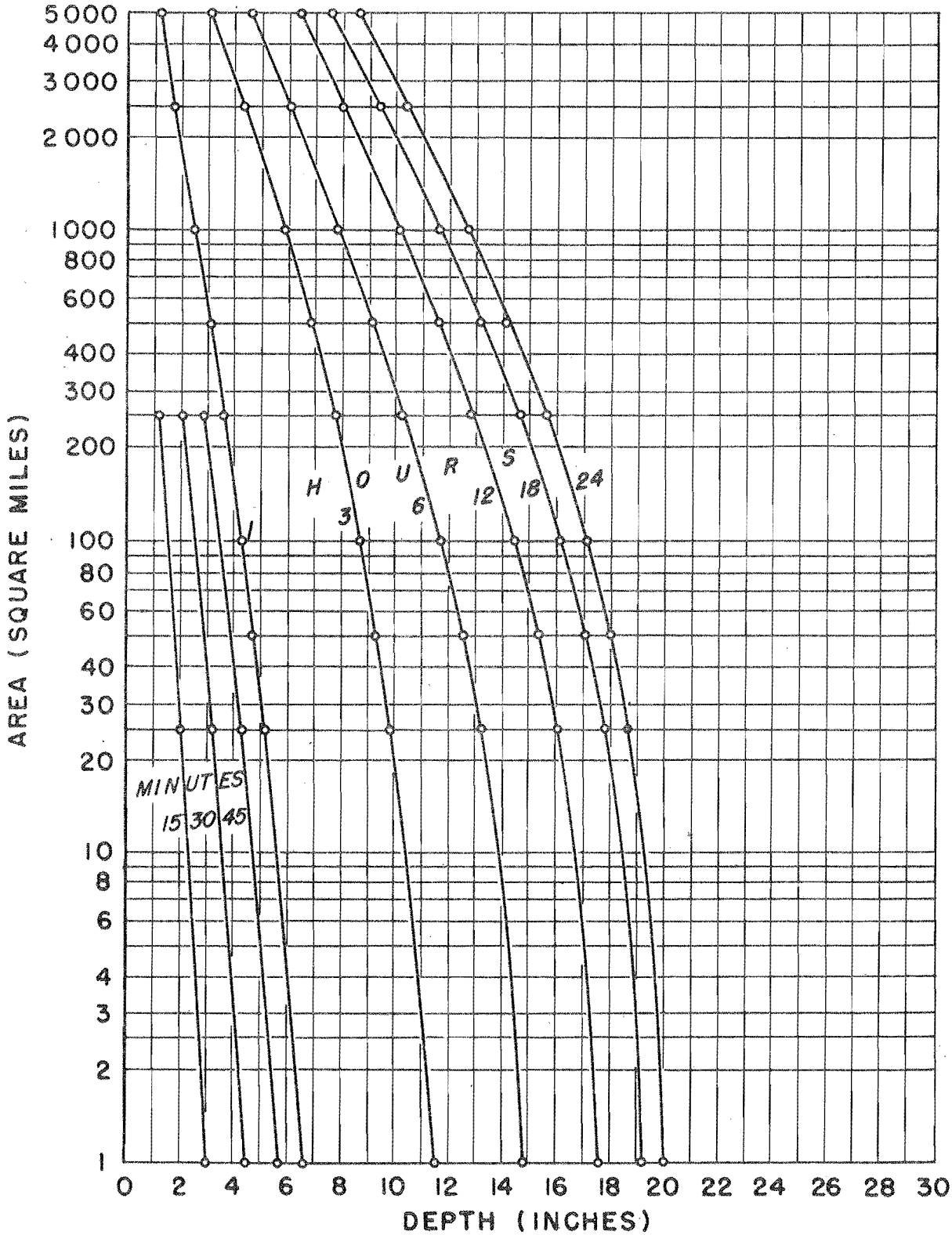

FILE 45044-1

FIGURE 12